NUCLEAR THEORY, Vol. 34 (2015)
eds. M. Gaidarov, N. Minkov, Heron Press, Sofia

Pairing-Quadrupole Connections in the Algebraic Shell Model Applied to sd-Shell Nuclear Systems

K.P. Drumev[1], **A.I. Georgieva**[2]

[1]Institute for Nuclear Research and Nuclear Energy, Bulgarian Academy of Sciences, Sofia 1784, Bulgaria

[2]Institute of Solid State Physics, Bulgarian Academy of Sciences, Sofia 1784, Bulgaria

Abstract. We present some particular applications within the algebraic realization of the Pairing-plus-Quadrupole /PQM/ for realistic sd-shell nuclear systems. The PQM uses the framework of the Elliott's SU(3) model. The probability distribution of the SU(3) basis states within the dynamical symmetries, corresponding to the isovector, isoscalar and total pairing eigenstates is obtained through a numerical diagonalization of the PQM Hamiltonian in each limit. This allows the investigation of the interplay between the pairing and quadrupole interactions in the Hamiltonian of the PQM. The relative strengths of the dynamically symmetric quadrupole-quadrupole interaction with the considered types of pairing interactions are investigated systematically. Specifically, we illustrate the evolution in the importance of different terms in the Hamiltonian by studying the chain of nuclei with 2 and 4 valence sd-shell particles going from the neutron-deficient to the neutron-rich part of the nuclear chart.

1 Introduction

The pairing [1] and the quadrupole-quadrupole [2] interactions are the most important short- and long-range interactions that have to be taken into account in the shell-model description of the nuclear systems [3]. In general, they dominate for nuclei with valence particles occupying different parts of the shell, but in many cases there are other characteristics, like the proton-neutron interactions or the isospin structure, that are also of great importance. This motivates the development of an extension of the Pairing-plus-Quadrupole Model /PQM/ [4] that also accounts for spin-isospin dependence of the nuclear excitation spectra.

The neutron deficient $N \sim Z$ nuclei are an interesting area for research with nuclei taking part in the rp-process of nucleosynthesis of the elements in nature. Here, the two modes – the pairing and the quadrupole interaction – compete. Moreover, interesting effects and the role of the isoscalar pairing can be studied as well. For these nuclei, full-space shell-model calculations are often difficult and lie beyond current computational capabilities. On the other hand,

symmetries may be present in some systems. Their importance lies in the fact that they allow for finding elegant solutions by offering a convenient choice of the basis turning the model space into one of a manageable size.

In this work, we describe the application of an extended algebraic realization [5] of the PQM theory for nuclei with two or four valence particles in the ds shell. The outline of perspectives and its future use for heavier shells and in two-shell model spaces is also discussed.

2 Algebraic Structure of the Pairing-plus-Quadrupole Model

2.1 Reduction schemes in the microscopic shell model

We start with a short explanation and analysis of the reduction schemes in Eqs. (1) and (2) below [5, 8], which give the reduction of the algebraic realization of the shell-model algebra.

$$
\begin{array}{lllll}
\{1^m\} & & U(4\Omega) & & \\
 & & \downarrow & & \\
\{\tilde{f}\} & [U(\Omega) & \otimes & U_{ST}(4)] & \{f\} \\
 & \downarrow \quad \searrow\ \alpha & & \downarrow & \\
[\tilde{\mu}] & [SO(\Omega) \quad [SU(3) & \otimes & SU_{ST}(4)] & \{f'\} \\
(\nu[p]) & \Leftrightarrow SO(8) \quad (\lambda,\mu) & & \sim SO(6) & [P] \\
\beta & \downarrow \quad \swarrow K & & \downarrow & \\
L & [SO_L(3) & \otimes & SU_S(2)] \otimes SU_T(2) & S,T \\
 & & \downarrow & \downarrow & \\
J & & SU_J(2) & \otimes SU_T(2) & T
\end{array}
\tag{1}
$$

$$
\begin{array}{llllll}
\{1^m\} & & & U(4\Omega) & & \\
 & & & \downarrow & & \\
\left\{\tilde{f}\right\} & [U(2\Omega) & & \otimes & U_T(2)] & \{f\} \\
 & \downarrow & & & \downarrow & \\
\langle\widetilde{\mu_s}\rangle & [Sp(2\Omega) & & \otimes & SU_T(2)] & T \\
 & \downarrow & \searrow^{\alpha} & & \downarrow & \\
[\widetilde{\mu_s}] & [SO(\Omega)\otimes SU_s(2)] & & [SU(3)\otimes SU_s(2)] & \otimes SU_T(2)] & T \\
 & \Leftrightarrow SO(5) & & (\lambda,\mu) & & \\
\beta & \downarrow & \swarrow_K & & \downarrow & T \\
LS & [SO_L(3) & \otimes & SU_s(2)] & \otimes SU_T(2)] & \\
 & & \searrow & & \downarrow & T \\
J & & & SU_J(2) & \otimes SU_T(2)] &
\end{array}
\tag{2}
$$

Equation (1) starts with the reduction of the shell model algebra

$$U(4\Omega) \supset U(\Omega) \otimes U_{ST}(4) \tag{3}$$

into the spatial $U(\Omega)$ and spin-isospin $U_{ST}(4)$ branches which are complementary [6]. The chain at the right-hand side of it

$$SU_{ST}(4) \supset SU_S(2) \otimes SU_T(2) \tag{4}$$

of the Wigner's supermultiplet model [7] gives the spin S and isospin T of the basis states of the shell model. In parallel to it, on the left-hand side we show the two possible reductions of the spatial part $U(\Omega)$ to the SO(3) algebra of the angular momentum. The middle chain [2]

$$U(\Omega) \supset SU(3) \supset SO_L(3) \tag{5}$$

defines the rotational limit of the model with only quadrupole-quadrupole interaction taken into account. The one on the left – through $SO(\Omega)$ whose representations are equivalent to the SO(8)-ones, which is the algebra of the isoscalar and isovector pairing interaction, defines the pairing limit of the shell-model algebra. Both these chains are complementary to the spin-isospin $U_{ST}(4)$ algebra. So, the important result, established in [8] is that the spatial subalgebra $U(\Omega)$ of the shell-model algebra $U(4\Omega)$ contains two distinct dynamical symmetries defined by the reduction chains: through $SO(\Omega) \sim SO(8)$ and through $SU(3)$.

Similarly, for the case when the pure isoscalar or isovector pairings are involved, we use the following reductions of $U(4\Omega)$ algebra:

$$U(4\Omega) \supset U(2\Omega) \otimes U_T(2) \supset [U(\Omega) \otimes U_S(2)] \otimes U_T(2) \tag{6}$$

$$U(4\Omega) \supset U(2\Omega) \otimes U_S(2) \supset [U(\Omega) \otimes U_T(2)] \otimes U_S(2) \tag{7}$$

The diagram given in Eq. (2) corresponds to the case of the pure isoscalar pairing. The pure isovector case is obtained by replacing S with T and vice versa. Using in this case the complementarity of $SO(\Omega) \sim SO_\sigma(5)$, where $\sigma = S \vee T$, we obtain the shell model pairing reductions that correspond to the well known three limits of the algebraic $SO(8)$ pairing model

$$\begin{array}{ccccc} & & SO(8) & & \\ & \swarrow & \downarrow & \searrow & \\ SO(6) & & SO_T(5) \otimes SO_S(3) & & SO_S(5) \otimes SO_T(3) \\ & \searrow & \downarrow & \swarrow & \\ & & SO_T(3) \otimes SO_S(3) & & \end{array} \tag{8}$$

2.2 Relation between the pairing and the $SU(3)$ basis states

Consequently, each pairing chain determines a full-basis set [9] that can be defined in the following way:

$$|\Psi_P\rangle \equiv |\{f\}, i, \beta L, S; JM\rangle\,, \tag{9}$$

where the set of quantum numbers $\{\mathrm{i}\}$ corresponds to the set of labels $\{\nu[p_1, p_2, p_3]\}$ of $SO(8)$ for the left branch of the reduction scheme in Eq. (1) and the left branch of (8) and to the set $\{\upsilon_S, t_S, \beta\}$ and $\{\upsilon_T, t_T, \beta\}$ for the isoscalar and isovector cases which correspond to the middle and right branches of (8). We choose to expand the states of the pairing bases (9), through the set of rotational basis states

$$|\Psi_R\rangle \equiv |\{f\}\alpha(\lambda, \mu)KL, S; JM\rangle\,, \tag{10}$$

since the microscopic $SU(3)$ model based on the three-dimensional harmonic oscillator has a well-developed theory, including the Wigner-Racah algebra for the calculation of matrix elements [10] in the $SU(3)$ basis. Hence, using the expansion

$$|\Psi_P\rangle_i = \sum_j C_{ij} \, |\Psi_R\rangle_j \, . \tag{11}$$

and the diagonalization procedure for the pairing interaction in the $SU(3)$ basis

$$\begin{aligned} \langle \Psi_P | H_{\text{pair}} | \Psi_P \rangle &= E_{\text{pair}}(m, i, [P], (ST)) \\ &= \sum_{jk} C^*_{ki} C_{ij} . \delta_{kj} . {}_k \langle \Psi_R | H_{\text{pair}} | \Psi_R \rangle_j , \end{aligned} \tag{12}$$

we obtain numerically the probability $|C_{ij}|^2$ with which the states of the SU(3) basis enter into the expansion of the pairing basis. This expansion could help evaluate the importance (weight) of the different $SU(3)$ states when we need to impose restrictions on the basis because of computational difficulties. Also, the known relations between the $SU(3)$ labels (λ, μ) and the β, γ shape variables of the geometrical model can be used for the analysis of the deformations of the pairing states.

2.3 The Hamiltonian of the PQM

For the purpose of our investigation we use the Hamiltonian

$$H = H_0 + V_{\text{res}} \tag{13}$$

of the PQM [11], where H_0 is the harmonic oscillator term or the single-particle interactions, that needs to be introduced when considering the shell plus orbital or the two-shell cases in order to place correctly the single-particle configurations with respect to each other. The residual interaction is used in the form

$$V_{\text{res}} = G_0 S^\dagger . S + G_1 P^\dagger . P - \frac{\chi}{2} Q . Q, \tag{14}$$

where the components of the quadrupole operator are

$$Q_\mu = \sum_l \sqrt{8(2l+1)} (a^\dagger{}_{l \frac{1}{2} \frac{1}{2}} \times \tilde{a}_{l \frac{1}{2} \frac{1}{2}})^{(200)}_{(\mu 00)} \tag{15}$$

and in (14) $Q.Q = 4C^2_{SU(3)} - 3L^2$ where the eigenvalue of the second invariant of $SU(3)$ is $C^2_{SU(3)} = \lambda^2 + \lambda\mu + \mu^2 + 3(\lambda + \mu)$. The pairing interactions in (14) are defined as

$$V_{\text{Pisc}} = G_0 S^\dagger . S \qquad \text{and} \qquad V_{\text{Piv}} = G_1 P^\dagger . P, \tag{16}$$

where

$$S^\dagger_\mu = \sum_l \beta_l \sqrt{\frac{2l+1}{2}} (a^\dagger{}_{l \frac{1}{2} \frac{1}{2}} \times \tilde{a}^\dagger_{l \frac{1}{2} \frac{1}{2}})^{(010)}_{(0\mu 0)} \tag{17}$$

and

$$P^{\dagger}_{\mu} = \sum_{l} \beta_l \sqrt{\frac{2l+1}{2}} (a^{\dagger}{}_{l\,\frac{1}{2}\,\frac{1}{2}} \times \tilde{a}^{\dagger}_{l\,\frac{1}{2}\,\frac{1}{2}})^{(001)}_{(00\mu)}. \tag{18}$$

The microscopic tensor operators (15), (17) and (18) are part of the $SU(\Omega)$ generators, since the operators $a^{\dagger}_{l\,\frac{1}{2}\,\frac{1}{2}}(a_{l\,\frac{1}{2}\,\frac{1}{2}})$ are creation (annihilation) operators of a nucleon on an orbit l, with spin $s = 1/2$ and isospin $t = 1/2$. The last two are part of the generators of the $SO(\Omega)$ and the $SO(8)$ algebras and their second order Casimir invariants are related. This allows us to investigate the influence of the different terms in the residual interactions on the spectra in real nuclear systems.

3 Calculations and Results

In this contribution, we present the application of the dynamical symmetries that were established in the Microscopic Shell Model in the ds shell for the even-even nuclei with 2 valence particles: ^{18}Ne and ^{18}O, and with 4 valence particles: ^{20}Ne as well as ^{20}O. The following observables are evaluated for the spectra of these nuclei: the root mean squared /RMS/ deviation of the model energies from the experimental ones $\sigma = \sqrt{\sum_i \left(E^i_{\text{Th}} - E^i_{\text{Exp}}\right)^2 / d}$ (per degree of freedom d), the weight of each of the isoscalar G_0, isovector G_1, and quadrupole χ interactions in the correct reproduction of the experiment. Also, information for the structure of the wave-function and/or B(E2) transitions may be added for best-fit values. We also aim to improve our best-fit results for the two-parameter Hamiltonian by considering the three-parameter case. The 4 valence-particle nucleus ^{20}Mg is excluded from our calculation because of not enough experimental states to be included in the RMS estimate.

To do our calculations, we work in the $SU(3)$ basis (10) which is generated by using the rules of $U(\Omega)$ to $SU(3)$ reduction (tabulated in the code [12]). Relying on tools developed to calculate reduced matrix elements for any type of physical operator between different $SU(3)$ irreps [13], we calculate the matrix elements of all the operators in this basis and then perform a numerical diagonalization to obtain the energy spectrum and the eigenstates.

3.1 Two-parameter results

The Hamiltonian we use for studying the energy spectrum of the considered realistic nuclear systems in the case of two parameters, can be written as

$$V_{\text{res}} = \frac{1}{2}(1-x)V_1 + \frac{1}{2}(1+x)V_2, \tag{19}$$

where x is called a control parameter. At $x = -1$ we have pure V_1 interaction and at $x = 1$ the limiting case of pure V_2 interaction is realized. We investigate in all cases the interrelations of the pairing interactions (16) on the quadrupole-

quadrupole interaction, hence $V_2 = -\frac{\chi}{2} Q.Q$. The pairing interactions could be

$$V_1 = V_{\text{Pt}} = G[S^\dagger.S + P^\dagger.P] \tag{20}$$

with $G_0 = G_1$, or $V_1 = G_0 S^\dagger.S$ and $V_1 = G_1 P^\dagger.P$. So, compared to the earlier $SU(3)$ one-shell realization [11, 14] of the PQM, we use a more general pairing Hamiltonian which includes proton-neutron pairing terms as well.

Now, let us use the energies of the low-lying states of the nuclear systems. In Figure 1, we present the results of a minimization procedure for the root-mean-squared /RMS/ value σ with respect to the two parameters G and χ of the residual interactions (19). The darker spots in the middle of the figures on the left present the intervals of change of the parameters for which we have the minimal values of σ or the values of the parameters fitted to a set of the lowest-lying positive-parity experimental energies E^i_{Exp} from the observed spectra [15] of a real nuclear system. The black dashed line in Figure 1(a), (c), (e), and (g) connects the values of each of the parameters G and χ at their respective limiting cases of pure pairing or pure quadrupole-quadrupole interactions. This line could be assigned as the axis of change of the parameter $-1 \leq x \leq 1$ as is used in Figures 1(b), (d), (f) and (h). The regions of the optimal values for the parameters lie on this line and their position in respect to its center could serve as a measure of the influence of each of the terms from the residual interactions on the energy spectra of the considered nucleus. An interesting observation from these two-parameter figures is that similar results for σ can be obtained by using various pairs of values (χ, G). This corresponds to somewhat different spectra in all these cases - from purely rotational to somewhat more pairing-like modes.

In the case of ^{20}Ne (see the upper three rows of Figure 1), the RMS estimate is performed over the 21 lowest-lying positive-parity experimental energies E^i_{Exp}. The results are given for the three choices of the pairing interaction - the isoscalar, the isovector, and the total pairing with a common strength parameter value. For this nucleus, we obtain a more rotational spectrum but observe a flat area of minima with similar RMS values of σ. The region of values suggesting reasonable description of the experiment do not reach the pure-pairing side. Using only the isoscalar or the isovector part of the pairing interaction, we obtain a spectrum where for pure pairing part of the degeneracy is lifted - either the 2^+_2 or the 0^+_2 state lies below the rest of the multiplet, respectively. The result for σ when we use the isoscalar interaction or the isovector pairing only is comparable with the one using the full pairing.

For the nucleus ^{20}O (where only the identical-particle isovector mode is present, thus $G_0 = 0$), similar values for σ are obtained for almost all the values of the parameter x (see Figure 1(g)). Also, the slope of change is bigger and the point of the best description shifts to the left towards a more pairing-like spectrum (see the position of the blue arrow in Figure 1(h) compared to the one in Figure 1(f). It is clear that complicated spectra observed in real nuclear systems are best reproduced by taking into account both the pairing and quadrupole-quadrupole interactions.

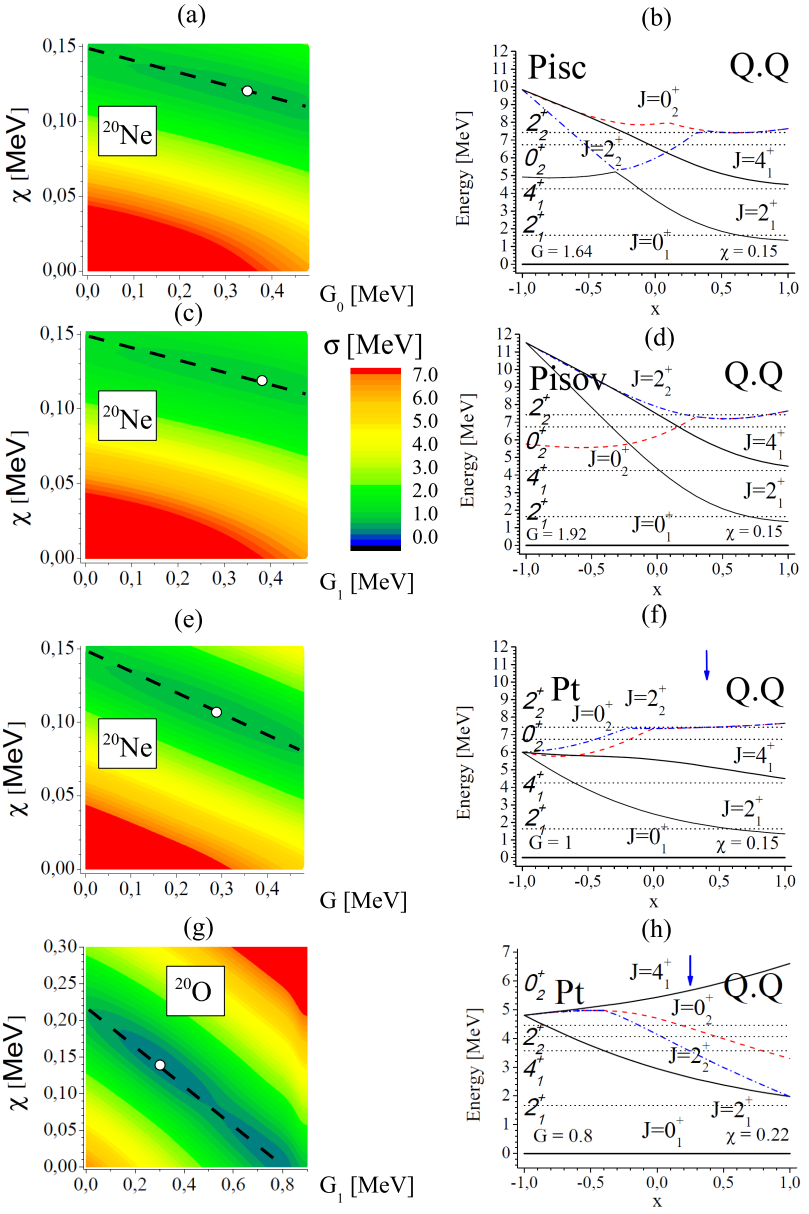

Figure 1. Results for the nuclei ^{20}Ne and ^{20}O with the Hamiltonians (19). (left) The absolute deviation σ in MeV for the excitation spectrum in the ds shell, calculated in full $SU3$ The white circles denote the position where σ is minimal. (right) Excitation spectrum of the lowest-lying energies with the control parameter x varying from -1 to 1 along the black dashed line from the corresponding figure on the left. The labels in italic and the dotted lines represent the experimental energies [15].

3.2 Three-parameter results and the phase transitions

Further, we can separate the two pairing modes - the isoscalar and the isovector one - and use a Hamiltonian (14). In this case, one has to introduce two control parameters y and z, described in detail in [16]. These are defined as having the following relation with the three strengths G_0, G_1 and χ of the Hamiltonian (14): $y = \chi/(\chi + G_1)$, $z = (\chi + G_1)/(\chi + G_0 + G_1)$ and the scaling parameter $c = \chi + G_0 + G_1$. Using them, the Hamiltonian becomes

$$H = c(1-z)S^{\dagger}.S + c(1-y)zP^{\dagger}.P - cyzQ.Q. \qquad (21)$$

The ratio between the best-fit values for the parameters χ, G_0 and G_1 can be ploted on a diagram resembling the Casten symmetry triangle, where each vertex represents one of the modes in pure form. The two control parameters y and z have the following meaning: an angle and a distance from the point of interest to one of the sides of the triangle, respectively (see Figure 2 below).

The three nuclei in the study (^{18}O, ^{18}Ne, and ^{20}O) have only one type of valence particles (protons or neutrons), so a three-parameter investigation is done only for the system ^{20}Ne. The best three-parameter results in this case are obtained for the values $\chi = 0.108$ MeV, $G_0 = 0.29$ MeV, and $G_1 = 0.29$ MeV, i.e. the addition of a third parameter does not change much the quality of description of the experimental results.

We also point out that if for the RMS estimate we use only 10 of the experimental states, the improvement in the σ result going from 2 to 3 parameter estimate is more pronounced. Also, in that case we obtain the following result for the strengths of the three interactions: $\chi = 0.102$ MeV, $G_0 = 0.04$ MeV, and $G_1 = 0.28$ MeV. This suggests that the ratio between two pairing modes changes and they are no longer equally present.

In Figure 2, the results obtained for all 4 nuclei in our study are illustrated. The outcome for the nuclei ^{18}O and ^{18}Ne has been obtained as the best two-

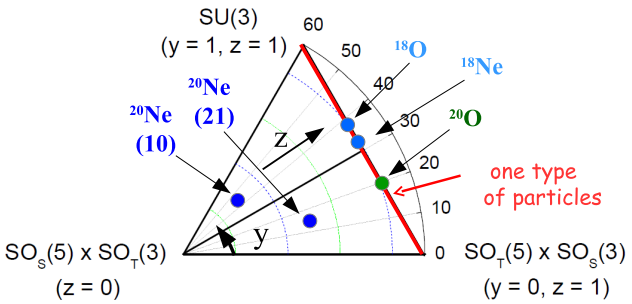

Figure 2. A symmetry triangle that illustrates the dominance of one of the interarctions - quadrupole-quadrupole, isoscalar pairing or isovector pairing. The coordinates of a point of interest are y and z. The five circles show the results for the nuclei ^{18}Ne, ^{18}O, ^{20}Ne, and ^{20}O.

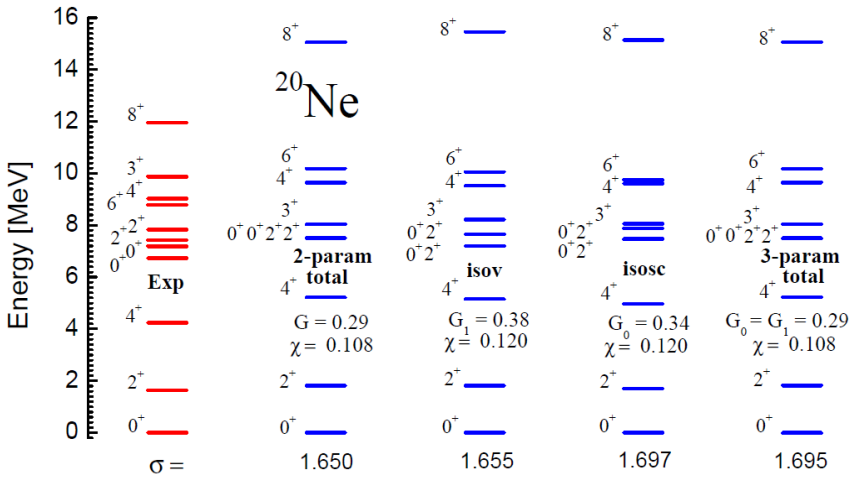

Figure 3. Comparison of the experimental and theoretical spectra obtained for ^{20}Ne with the Hamiltonians $V_{\text{Pisc}} - \frac{\chi}{2}Q.Q$, $V_{\text{Piv}} - \frac{\chi}{2}Q.Q$, and $V_{\text{Pisc}} + V_{\text{Piv}} - \frac{\chi}{2}Q.Q$. Below each spectrum, the RMS value σ obtained has been written. The three-parameter result has a slightly bigger σ value since the best values remain the same, while the degrees of freedom are one less.

parameter estimate using the Hamiltonian with the isovector pairing only. The cases of no isoscalar pairing involved (which happens when one type of valence particles is present in the system) lie along the $SO_T(5)$-$SU(3)$ line. Moreover, the nucleus expected to be more collective ^{20}O (the experimental energy ratio $E_4/E_2(exp) = 2.13$) turns out to be positioned closer to the $SO_T(5) \times SO_S(3)$ vertex of the triangle. The theoretical result for the ratio is a reasonable one (E_4/E_2(th) $= 2.14$). The result for the nuclei ^{18}Ne (E_4/E_2(exp) $= 1.79$) and ^{18}O (E_4/E_2(exp) $= 1.79$) are E_4/E_2(th) $= 2.53$ and E_4/E_2(th) $= 2.77$ which is related to their position closer to the $SU(3)$ vertex in the figure. Only the ^{20}Ne (E_4/E_2(exp) $= 2.6$) result for the parameters lies inside the triangle and the ratio obtained with the best 3-parameter estimate is E_4/E_2(th) $= 2.86$. The result, obtained for the 10 experimental states, namely the low-lying states $0_2^+, 0_3^+, 2_1^+, 2_2^+, 2_3^+, 3_1^+, 4_1^+, 4_2^+, 6_1^+, 8_1^+$, is also shown in the figure and is positioned closer to the vertex of the isoscalar pairing.

Finally, in Figure 3, a comparison between excitation spectra calculated for ^{20}Ne has been done. The deviation from the experimental energy spectrum is reduced once one goes from two-parameter to three-parameter description, result more clearly seen for the case of the 10 low-lying experimental states. In that case we obtain the following result for the strengths of the three interactions: $\chi = 0.102$ MeV, $G_0 = 0.36$ MeV, and $G_1 = 0.04$ MeV. This suggests that the ratio between the two pairing modes changes and they are no longer equally present. We also observe that in the isoscalar and the isovector case the

degeneracy of the states 0_2^+, 0_3^+, 2_2^+, and 2_3^+ is partially removed as is in the experiment.

In principle, we can use a different statistics in the minimization procedure, namely a modified root-mean-squared /RMS/ estimate of the form $\sigma_1 = \sqrt{\sum_i \left(E^i_{\rm Th} - E^i_{\rm Exp}\right)^2 / {E^i_{\rm Exp}}^2 d}$ (per degree of freedom d) with respect to the two parameters G and χ of the residual interactions (19). Here, the experimental energies are also included to weigh each theory from experiment difference. Then, the minimum is achieved at $\chi = 0.105$ MeV and $G = 0.22$ MeV. In this case, the state 2_1^+ differs by only 4% from the experimental state whereas the σ estimate gives a 16% discrepancy. The numbers for the 4_1^+ state are 9% versus 25%, while for the 8_1^+ state they are 16% and 26%, respectively. In conclusion, the σ_1 estimate favors a more accurate description (i.e. lower percent difference) in the lower-lying states. While the theoretical results lie closer to the experimental energies, the $E(4)/E(2)$ ratios become more poorly estimated.

4 Conclusion

On the basis of the algebraic reductions of the spatial part of the shell-model algebra $U(4\Omega)$ through the dynamical symmetries defined by the microscopic pairing algebras, containing pure isoscalar ($T = 0, S = 1$), pure isovector ($T = 1, S = 0$), total pairing interaction with both of them with equal strenghts and Elliott's $SU(3)$ algebra, we elucidate the algebraic structure of an extended Pairing-plus-Quadrupole Model, in the framework of the SU(3) scheme [6]. The four reduction chains appear as distinct dynamical symmetries of the shell-model algebra. This allows us to study the complementarity and competitive effects of the quadrupole-quadrupole and pairing interactions on the energy spectra of the nuclear systems. The theoretical results are compared with experimental energy spectra of the nuclei ^{18}Ne, ^{18}O, ^{20}Ne, and ^{20}O, from where the optimal values of two and three parameters of the residual interactions are obtained. A more accurate description of the interplay between the PQM's interactions is obtained in the three-parameter fit to the experiment.

A further and natural development of this model is its realization in more than one shell. Some steps have already been done in this direction [5] but one should be cautious with the choice of nuclei to be studied and the model spaces to work in. The reason is that one has to deal with the center-of-mass effects [17] that should be addressed appropriately since they can be severe. A favorable choice for such calculations would be the $s_{1/2}d_{3/2} + f_{7/2}$ or $s_{1/2}d_{3/2} + fp$ (which realizes as $pseudo - p + f_{7/2}$ or $pseudo - p + fp$ in $SU(3)$ language) model spaces. This implies the systems of interest to be nuclei like the four-particle $N = Z$ system ^{32}S or the eight-particle one ^{36}Ar.

Acknowledgements

This work was supported by the Bulgarian National Foundation for Scientific Research under Grant Number DFNI-02-6/12.12.2014.

References

[1] B.H. Flowers, *Proc. Roy. Soc. London, Ser. A* **212** (1952) 248.

[2] J.P. Elliott, *Proc. Roy. Soc. London, Ser. A* **245** (1958) 128; **245** (1958) 562.

[3] A. Bohr, B.R. Mottelson, and D. Pines, *Phys. Rev.* **110** (1958) 936.

[4] S.T. Belyaev, *Mat. Fys. Medd. Dan. Vid. Selsk.* **31** No. 11 (1959); L.S. Kisslinger and R.A. Sorensen, *Rev. Mod. Phys.* **35** (1963) 853; M. Baranger and K. Kumar, *Nucl. Phys.* **62** (1965) 113.

[5] K.P. Drumev, A.I. Georgieva, NUCLEAR THEORY, Vol. **33** (2014) 162, Proceedings of the 33 International Workshop on Nuclear Theory, 22-28 June 2014, eds. A. Georgieva, N. Minkov, Heron Press, Sofia.

[6] J.P. Draayer, In: "*Algebraic Approaches to Nuclear Structure: Interacting Boson and Fermion Models*", Contemporary Concepts in Physics VI, edited by R.F. Casten (Harwood Academic, Chur, Switzerland, 1993).

[7] E.P. Wigner, *Phys. Rev.* **51** (1937) 106.

[8] K.P. Drumev, A.I. Georgieva, NUCLEAR THEORY, Vol. **32** (2013) 151, Proceedings of the 32 International Workshop on Nuclear Theory, 24-29 June 2013, eds. A. Georgieva, N. Minkov, Heron Press, Sofia.

[9] V.K.B. Kota, J.A. Castilho Alcaras, *Nucl. Phys.* **A764** (2006) 181.

[10] Y. Akiyama and J.P. Draayer, *Comput. Phys. Commun.* **5** (1973) 405.

[11] C. Bahri, J. Escher, and J.P. Draayer, *Nucl. Phys.* **A592** (1995) 171.

[12] J.P. Draayer, Y. Leschber, S.C. Park, and R. Lopez, *Comput. Phys. Commun.* **56** (1989) 279.

[13] C. Bahri, J.P. Draayer, *Comput. Phys. Commun.* **83** (1994) 59.

[14] C.E. Vargas, J.G. Hirsch, J.P. Draayer, *Nucl. Phys.* **A690** (2001) 409.

[15] http://www.nndc.bnl.gov/

[16] J. Cseh, J. Darai, arXiv:1404.3503v1[nucl-th].

[17] J.P. Elliott and T.H.R. Skyrme, *Proc. Roy. Soc. London, Ser. A*, **232** (1955) 561.